Electric Power Systems Research 208 (2022) 107910

Contents lists available at ScienceDirect

Electric Power Systems Research

journal homepage: www.elsevier.com/locate/epsr

Self-organized Partition of Distribution Networks with Distributed Generations and Soft Open Points

Li Ma, Lingfeng Wang *, Zhaoxi Liu

Department of Electrical Engineering and Computer Science University of Wisconsin-Milwaukee, Milwaukee, WI 53211 USA

ARTICLE INFO

Keywords:
Self-organized network partition
Resilience improvement
Distribution network
Soft open point
Bi-objective discrete game

ABSTRACT

Islanding operation relying on distributed generations (DGs) is anticipated to be a promising operational measure for resilience enhancement of distribution networks. In this paper, a self-organized network partition framework for controllable DGs (CDGs) is proposed for the distribution network with DGs and soft open points (SOPs) from a game-theoretic perspective. The labeled numbers of the nodes on paths between every two adjacent CDGs are used as the optimization variables in the partition formation, which can avoid a large number of invalid partition schemes. Two objectives including the weighted recovered load and the power loss are considered, which reflect the goals of maximizing the critical load recovery and minimizing the power loss, respectively. The power loss is determined through the AC power flow calculation using Newton-Raphson method considering the operational characteristics of SOPs. The partition problem is modeled as a discrete bi-objective game, which is further transformed into a continuous game model, and the existence of the Pareto-Nash equilibrium is also proved. A decentralized method is developed to solve the proposed bi-objective game relying on the local communications and a global information discovery scheme, which is more practical after the extreme events. Numerical studies on the IEEE 69-bus distribution system and a 135-bus multi-feeder system are performed to validate the effectiveness of the proposed method. The proposed model is applied in different network topologies, and compared with the centralized optimization models. The robustness of the method to communication failures is analyzed, and the scalability of the proposed model is also validated through testing it in a larger distribution network.

1. Introduction

Power system outages caused by extreme weather conditions and man-made threats (e.g., cyberattacks) could have significant adverse effects on societal development and human daily life [1,2]. Such extreme events are expected to be even more frequent and more disastrous as climate change aggravates natural hazards such as earthquakes, deep freeze, hurricanes, tornadoes, floods, and wildfires. Meanwhile, the increasing applications of information and communication technologies (ICTs) are introducing a wide range of cyber vulnerabilities to modern power grids. Resilience study against such potential catastrophic power outages has attracted growing attention worldwide recently. Resilience is defined as the ability of the system to reduce the magnitude and/or duration of disruptive events, which dictates the capability to anticipate, absorb, adapt to, and/or rapidly recover from a potentially disruptive event [3].

The growing penetration of distributed generation (DG) has greatly promoted the research on the resilience improvement of distribution systems [4]. The related studies have been performed mainly based on the hardening measures [5,6], operational measures[7–12], and the combination of these two measures [13–16]. The hardening measures mainly refer to the physical upgrades of the infrastructure [17], including upgrading the lines and poles, optimally allocating DGs, etc. These measures usually need a massive investment. For the operational measures, islanding operation relying on DGs is a promising technique to improve the system resilience [18], and the related research covers both centralized models[7,8] and decentralized models [10,11]. In [10], a distributed multi-agent coordination scheme was designed, and the switches were equipped with local communication capabilities within mature short-range wireless networks such as Wi-Fi and ZigBee. The impacts of vehicle-to-grid (V2G) facilities were considered in the service restoration in [11]. In [12], a multi-resource resilience enhancement approach was designed to assist system operators in decision-making against extreme weather events, based on fully coordination of DGs, mobile emergency generators, remote-controlled switches, manual switches and operation crew teams in the system. For the hybrid

* Corresponding author.
E-mail address: wang289@uwm.edu (L. Wang).

https://doi.org/10.1016/j.epsr.2022.107910
Received 21 September 2021; Received in revised form 19 January 2022; Accepted 6 March 2022

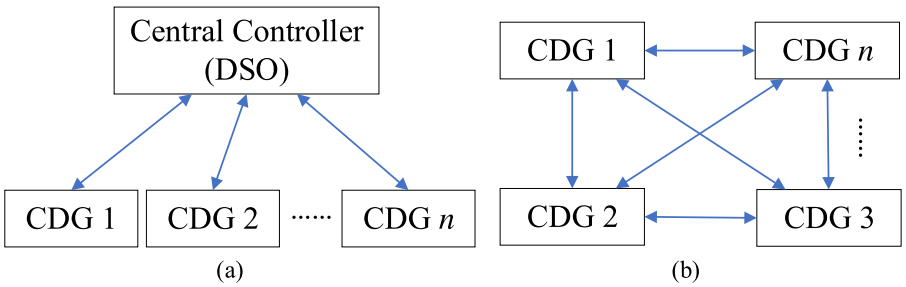

Fig. 1. Frameworks of the network partition model: (a) A centralized framework, and (b) A self-organized framework.

measures, the hardening plan and operational restoration measures are integrated in a tri-level defender-attacker-defender model considering the malicious attacks in [13]. In [14], a two-stage framework including pre-restoration and dynamic dispatch of the mobile power sources and network configuration is proposed for system recovery enhancement. The investment optimization of the mobile energy storage (ES) and the re-routing problem of the installed mobile ES are considered together in [15] to reduce the expected load shedding caused by disasters. An optimal framework for the resilience-oriented design for distribution networks to protect against extreme weather events was proposed in [16], through minimizing the summation of hardening cost, operation cost, and load shedding cost. In addition, for the effect of DGs on the protection system, the fault direction identification method and optimum overcurrent protection for deregulated distribution networks containing parallel feeders were studied in [19].

As the location and capacity of the DGs are relatively fixed in the operational measures, DGs are hampered by these constraints to further enhance the resiliency of distribution systems. In recent years, the advanced power electronics based technologies have provided promising opportunities to address this issue. The concept of soft open point (SOP) proposed in [20] is expected to benefit distribution systems in various aspects such as power loss reduction, feeder load balancing, voltage profile improvement, and DG integration, so the SOP technology is regarded as an emerging solution to fill the gap in this area. Although SOP is a new type of intelligent power distribution device, the main components of SOP are mature technologies given the commercial availability of power electronic converters [21]. SOPs used in the existing studies are mainly built with fully controlled power electronic devices, and back-to-back (B2B) voltage source converters are the most widely adopted technology [22,23]. SOPs are able to regulate the power on the connected line accurately and responsively, and provide voltage support for connected loads. In addition, the deployment of SOPs changes the topology of distribution network from the radial to meshed configuration, which provides more alternative network schemes for resilience improvement. Some work was carried out considering SOPs in the process of islanding partition in [24], where the power loss of SOPs was modeled as a fixed coefficient.

In the existing studies on islanding partition, the optimization objectives mainly focused on maximizing the amount of recovered load after power outage [7,8,10,11,24], while some studies also minimized the number of islands [7] and reduced the switching operations [11]. However, the power loss in the partitions, which is also affected by the network topology and influences the load recovery to some extent, has not been considered. In addition, there are two main types of variables involved in the partition decision, i.e., the states of lines and the divisions of nodes. When only using these two types of variables, a number of invalid partition schemes may be generated due to the topology limitations. To address these issues, this paper proposes a bi-objective partition optimization model for the distribution network with DGs and SOPs, considering the objective of power loss in the partitions. Meanwhile, a new type of variables is introduced in the optimization process to reduce the invalid strategy set. The operational characteristics of SOPs are integrated into the power flow formulation with great details. The main contributions and advantages of this paper are listed as follows.

(1) A self-organized partition framework for resilience enhancement of distribution networks is developed based on the bi-objective discrete game theory. The game theory method is applied in the distribution network partition problem involving physical changes of the network topology, which is different from existing studies where the physical networks are usually unchanged.
(2) A decentralized realization for solving the bi-objective game is proposed based on the local communications through global information discovery scheme. In the proposed model, each CDG only needs to communicate and coordinate with its adjacent load nodes and CDGs.
(3) Relying on the local communications and global information discovery scheme, the proposed model is more reliable when failures occur in the communication network as compared with a centralized optimization model. The robustness analysis of the model to communication failures is also performed.

The rest of the paper is organized as follows. The self-organized network partition framework is introduced in Section II. The methods for strategy sets determination and objective calculation are presented in Section III. The discrete bi-objective game model is proposed in Section IV, and the equivalence, equilibrium existence and decentralized solving procedure of the game are also presented in this section. In Section V, numerical case studies on the IEEE 69-bus distribution system and a 135-bus multi-feeder system are performed to validate the effectiveness of the proposed model and solution. Finally, conclusions are drawn in Section VI.

2. Self-organized Network Partition Framework

In the face of a power outage, if the central controller and its communication system are in normal conditions, network partition optimization can be performed by the distribution system operator (DSO) in a centralized manner with the aid of the controller. As shown in Fig. 1 (a), all CDGs can communicate with the DSO – the required information is transferred to the central controller from the CDGs and users while the optimized partition schemes are fed back to CDGs.

However, in the catastrophic events, the communication links for the central controller may be compromised, and centralized optimization may not be implementable. In this case, optimization relying on local communications is a more viable solution, and the global information discovery scheme in [10] is adopted in our work. In this paper, a self-organized partition framework is developed utilizing local communications, as shown in Fig. 1 (b). The CDGs can communicate with each other with the help of switches supporting local communication functionality, as described in [10]. Assuming the CDGs are rational participants and a better performance means more profits, each CDG would strive to optimize the performance of its own partition. Each CDG's partition formation and corresponding performance are greatly affected by its adjacent CDGs' strategies due to the topology limitation

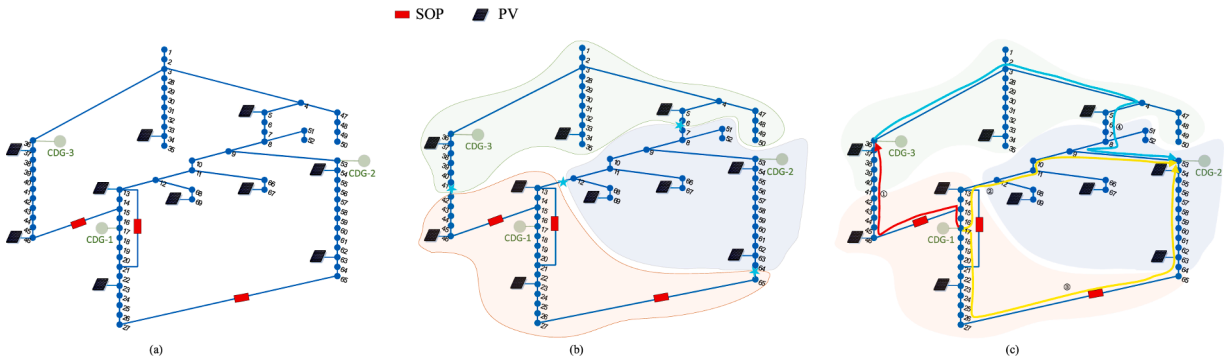

Fig. 2. Optimization strategy selection.

and user positions and behaviors. As an effective tool to model the interaction among rational, mutually aware players whose payoffs are impacted by other plays' decisions [25], game theory is used here to provide a practical solution of partition optimization under the self-organized framework, and the solving process is performed in a decentralized manner.

In this study, two objectives are considered in the partition decision. The first objective is to maximize the amount of recovered loads in the partition and the second one is to minimize the power loss in the partitions. The former also considers the importance levels of the loads in the distribution network, as critical loads need to be first recovered with limited generation resources. The latter is helpful to reflect the proximity principle of power supply on the one hand, as a longer supply distance usually results in higher line losses and worsened voltage quality. On the other hand, less power loss also means more load can be recovered with limited generation resources in an emergency. Therefore, the power loss is included in the objective of the proposed optimization model.

For simplicity, it is assumed that only one CDG is considered in each partition in this paper. However, the proposed models are also applicable to the situations with multiple CDGs in a partition. This could be implemented in two ways. One way is regarding a group of separate CDGs as one CDG in the partition if they are close to each other and an appropriate coordinating strategy is available between them. Another way is selecting part of the CDGs with larger generating capacities as the executable CDGs in the partition, while the other small-scale CDGs are set as PQ nodes (with fixed generation), just similar to the nodes with uncontrollable DGs.

3. Strategy Set and Objectives

3.1. Selection of Strategy Set

As presented in Section 2, CDGs are the main executors and participants of the partition optimization, which is to determine which nodes (including the nodes installed with uncontrollable DGs, such as PVs in this paper) will be grouped with each CDG to form the partition. Intuitively, the decision variables can be set as the index of the CDG with which each load node is grouped. However, if there are N nodes and G CDGs in the distribution network, the total number of partition schemes is up to G^N. Taking the IEEE 69-bus system in Fig. 2 (a) as an example, we have $G^N = 3^{66} = 3.09 \times 10^{31}$. Actually, most strategies in this solution set are not valid in practice due to the network topology constraint. To deal with this issue, a strategy reduction method is proposed using a new type of variable so that most of the invalid strategies can be excluded.

In the proposed method, the nodes in the distribution network are first divided into G partitions based on the proximity principle (according to the electrical distance), which dictates each node is grouped with the closest CDG to form the partitions, as shown in Fig. 2 (b). Then based on the border edges between the partitions (marked with blue stars in Fig. 2 (b)), the paths connecting two CDGs can be determined as shown in Fig. 2 (c) (each path only get through one blue star). There are 4 paths in the case as shown in Fig. 2 (c), and the new variables are set as the labeled numbers on the paths. For CDG-1, 3 paths are involved, which means 3 variables should be set for CDG-1. Similarly, there are 3 and 2 variables for CDG-2 and CDG-3, respectively. Taking path ① as an example, there are 12 nodes on the path (including nodes 16,15,46,45,44,43,42,41,40,39,38,37), then the variable can be assigned a number in [1,2,3,4,5,6,7,8,9,10,11,12], which is the node's labeled number on this path. It should be noticed that the children nodes will not appear on the paths, and they will choose the same CDG as their root nodes. For example, nodes 68 and 69 will join the same CDG as node 12. For the CDG-1, the nodes from the first to the n_{1i}-th on the path will be assigned to CDG-1's partition, while the nodes from the n_{3i}-th to the 12-th on the path will join CDG-3's partition. n_{1i} and n_{3i} are the variables for CDG-1 and CDG-3 on the previously mentioned path. Using this method, there are 2.8×10^6 partition strategies when half of the nodes on all paths are considered selectable. The strategy number has been drastically reduced compared with the original number 3.09×10^{31}.

3.2. Calculation of Objective Functions

In this section, the calculation methods for each objective of a given partition will be described in detail. The first objective to maximize the weighted recovered load is solved based on a linear integer programming model. The second objective is the power loss in a partition. The i-th CDG is denoted as G_i with the maximum power output $C_i, i \in \{1,2,\ldots, p\}$. A set of user nodes $V = \{v_1, v_2, \ldots, v_n\}$ corresponds to the load set $l = \{l_1, l_2, \ldots, l_n\}$, and V_i denotes the set of user nodes in the i-th partition, i.e., the partition with the i-th CDG.

1) Weighted recovered load

The recovered nodes within a partition can be determined by solving the following integer programming problem:

$$\begin{aligned} &max \sum_{u \in V_i} L_{ui} l_u A_u \\ &s.t. \sum_{u \in V_i} L_{ui} l_u \le C_i \end{aligned} \tag{1}$$

where L_{ui} is the integer variable indicating if the u-th load node within the i-th partition is recovered, and $L_{ui} = 1$ when the u-th load node is recovered, otherwise $L_{ui} = 0$; and A_u indicates the importance level of the u-th load node, and it is determined based on the user category at the u-th node. The more important the user is, the larger A_u should be set. The important users mainly include hospitals, government offices, banks, data centers, etc. For simplicity, A_u can be set as either 1, 2, or 3 in our study. The constraint in (1) implies that the load nodes recovered in the i-th partition should not exceed the maximum output of the i-th CDG. It is also assumed the nodes with redundant PV/RES must be

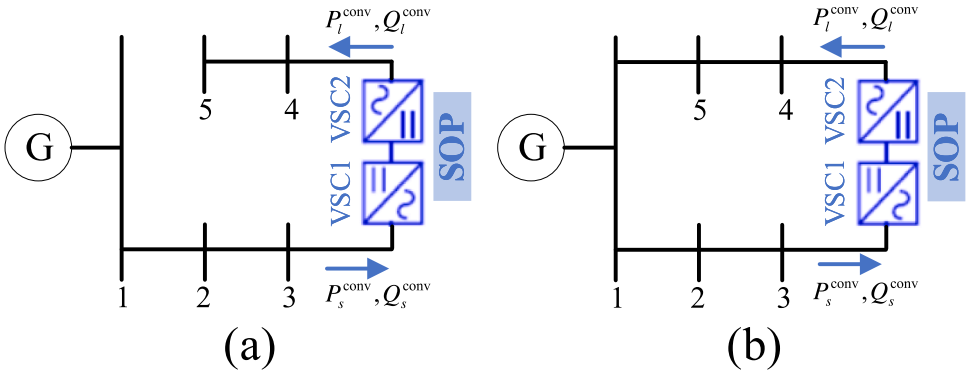

Fig. 3. Different topologies with SOPs: (a) Radial, (b) Meshed.

Table 1
Control strategies of SOPs with different topologies

Topology	Converter	Control mode	Given	Unknown
Radial	VSC1	Q	Q_s^{conv}	$v_s, \theta_s, P_s^{\text{conv}}$
	VSC2	VV_{dc}	v_l, θ_l	$P_l^{\text{conv}}, Q_l^{\text{conv}}$
Looped	VSC1	PQ	$P_s^{\text{conv}}, Q_s^{\text{conv}}$	v_s, θ_s
	VSC2	QV_{dc}	Q_l^{conv}	$v_l, \theta_l, P_l^{\text{conv}}$

restored.

2) Power loss

Based on the first objective, the nodes in the partition to be recovered are determined, and the power loss can then be calculated based on this result. The power loss is determined according to the power flow analysis, and the SOPs are considered in the power flow model. The power flow model in [26] is modified and used in this paper, which guarantees the power balance between the load and generation within each partition. For the SOPs in the partition of a CDG, only two topologies, i.e., radial and meshed networks, are possible as shown in Fig. 3. Different control strategies should be adopted for SOPs according to the network topology as shown in Fig. 3, and which topology will be chosen is determined by the partition scheme. When the SOP in a partition scheme is included in a loop, the meshed topology is considered; when the SOP in a partition scheme is not in a loop, the radial topology is considered. The control modes, along with the given and unknown variables for each converter of the SOPs in different network topologies, are listed in TABLE 1 (In Fig. 3, subscripts s and l in TABLE 1 correspond to nodes 3 and 4, respectively). For the SOP in the meshed topology, VSC1 is set to regulate active and reactive power (PQ mode) and VSC2 is set to regulate the dc-link voltage and control reactive (QV_{dc} mode). For the SOP in the radial topology, the l-th node is a slack bus, so v_l, θ_l should be given, and Q_l^{conv} is unknown to control the voltage. P_l^{conv} is unknown as it depends on the losses in the network connected to the l-th node, and only Q_s^{conv} is given. More detailed explanations on the control mode coupled with the given and unknown variables can be found in [26].

The equivalent model for an SOP is represented by the middle two blocks in Fig. 4. In Fig. 4, only nodes s and l which are connected to the converters of SOP are shown in the figure, and other nodes are not shown for the sake of clarity. The set of power balance equations for non-slack nodes and non-voltage controlled nodes is given as follows:

For the nodes connected to the SOP:

$$g_s^P = P_s - \left(P_s^{\text{gen}} - P_s^{\text{load}} - P_s^{\text{conv}}\right) = 0 \tag{2}$$

$$g_s^Q = Q_s - \left(Q_s^{\text{gen}} - Q_s^{\text{load}} - Q_s^{\text{conv}}\right) = 0 \tag{3}$$

$$g_l^P = P_l - \left(P_l^{\text{gen}} - P_l^{\text{load}} + P_l^{\text{conv}}\right) = 0 \tag{4}$$

$$g_l^Q = Q_l - \left(Q_l^{\text{gen}} - Q_l^{\text{load}} + Q_l^{\text{conv}}\right) = 0 \tag{5}$$

For the nodes not connected to the SOP:

$$g_i^P = P_i - \left(P_i^{\text{gen}} - P_i^{\text{load}}\right) = 0 \tag{6}$$

$$g_i^Q = Q_i - \left(Q_i^{\text{gen}} - Q_i^{\text{load}}\right) = 0 \tag{7}$$

where $P_*^{\text{gen}}/Q_*^{\text{gen}}$ is the active/reactive power of the generation at the node, $P_*^{\text{load}}/Q_*^{\text{load}}$ is the active/reactive power of the load, and $P_*^{\text{conv}}/Q_*^{\text{conv}}$ is the active/reactive power of the converters in the SOP. P_i and Q_i represent the active and reactive power injected into the grid at node i, respectively:

$$P_i = V_i \sum_{k \in \mathcal{N}_i} V_k [G_{ik}\cos(\theta_{ik}) + B_{ik}\sin(\theta_{ik})] \tag{8}$$

$$Q_i = V_i \sum_{k \in \mathcal{N}_i} V_k [G_{ik}\sin(\theta_{ik}) - B_{ik}\cos(\theta_{ik})] \tag{9}$$

where $\mathcal{N}_i$ represents the set of adjacent nodes to node i, $\theta_{ik} = \theta_i - \theta_k$ is the phase difference between nodes i and k, and $G_{ik} + jB_{ik}$ represents the admittance of the line between nodes i and k. P_s, Q_s, P_l and Q_l in (2)-(5) can also be represented using the similar expressions as (8) and (9).

For the back-to-back (BTB) converter based SOP, the power balance equation g_{conv}^P reflects the relationship between P_s^{conv} and P_l^{conv}

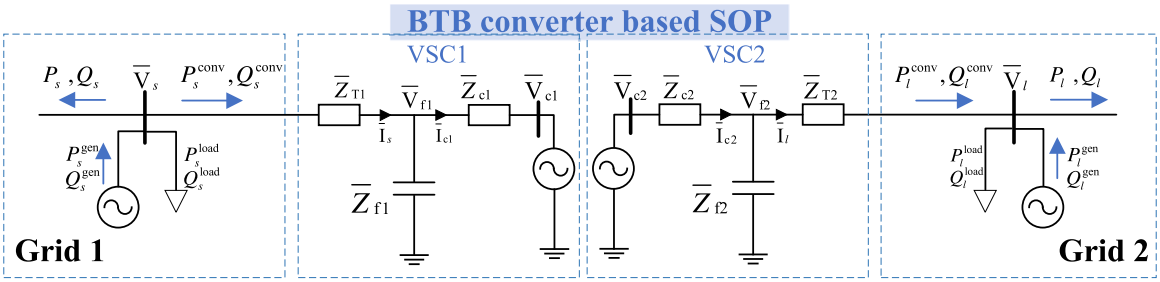

Fig. 4. The schematic diagram for the power flow balance.

considering the Joule and switching losses:

$$g_{\text{conv}}^{P} = P_{l}^{\text{conv}} + P_{\text{J2}} + P_{\text{Sw2}} + P_{\text{J1}} + P_{\text{Sw1}} - P_{s}^{\text{conv}} = 0 \tag{10}$$

$$P_{\text{J1}} = I_{s}^{2} R_{\text{T1}} + I_{\text{c1}}^{2} R_{\text{c1}} \tag{11}$$

$$P_{\text{Sw1}} = a_0 + a_1 I_{\text{c1}} + a_2 I_{\text{c1}}^{2} \tag{12}$$

$$P_{\text{J2}} = I_{l}^{2} R_{\text{T2}} + I_{\text{c2}}^{2} R_{\text{c2}} \tag{13}$$

$$P_{\text{Sw2}} = a_0 + a_1 I_{\text{c2}} + a_2 I_{\text{c2}}^{2} \tag{14}$$

where R_{T1}, R_{T2}, R_{c1} and R_{c2} are the winding resistances and a_0, a_1, and a_2 are the given coefficients. According to [26], I_s, I_{c1}, I_l and I_{c2} are the functions of P_s^{conv}, P_l^{conv}, Q_s^{conv}, Q_l^{conv}, V_l and V_s, which can be derived from the model shown in Fig. 4. The constraints for the SOP operation including the limits for the root mean square (RMS) converter current, coupled with the RMS converter voltage and reactive power absorbed by the converter are represented as follows:

$$I_{\text{c1}} \le I_{\text{c}}^{\max}, I_{\text{c2}} \le I_{\text{c}}^{\max} \tag{15}$$

$$V_{\text{c1}} \le k_m V_{\text{dc}}, V_{\text{c2}} \le k_m V_{\text{dc}} \tag{16}$$

$$Q_{s}^{\text{conv}} \le k_Q S_{\text{SOP}}, Q_{l}^{\text{conv}} \ge -k_Q S_{\text{SOP}} \tag{17}$$

where $I_{\text{c}}^{\max}$ is the upper bound of the RMS converter current, k_m is a coefficient depending on the pulse-width modulation (PWM), V_{dc} is the voltage across the dc-link capacitor, S_{SOP} is the capacity of the SOP, and k_Q is a specific coefficient.

There can be multiple SOPs in one partition at the same time, and (2)-(5) can be applied for the power flow formulation of other SOPs. The Newton-Raphson method is used here to solve the power flow calculation, and the following expression is used to update the mentioned unknown variables:

$$\begin{bmatrix} \frac{\partial \mathbf{g}^{P}}{\partial \boldsymbol{\theta}} & \frac{\partial \mathbf{g}^{P}}{\partial \mathbf{v}} & \frac{\partial \mathbf{g}^{P}}{\partial \mathbf{P}_s} & \frac{\partial \mathbf{g}^{P}}{\partial \mathbf{P}_l} \\ \frac{\partial \mathbf{g}^{Q}}{\partial \boldsymbol{\theta}} & \frac{\partial \mathbf{g}^{Q}}{\partial \mathbf{v}} & 0 & 0 \\ 0 & \frac{\partial \mathbf{g}_{\text{conv}}^{P}}{\partial \mathbf{v}} & \frac{\partial \mathbf{g}_{\text{conv}}^{P}}{\partial \mathbf{P}_s} & \frac{\partial \mathbf{g}_{\text{conv}}^{P}}{\partial \mathbf{P}_l} \end{bmatrix} \begin{bmatrix} \Delta\boldsymbol{\theta} \\ \Delta\mathbf{v} \\ \Delta\mathbf{P}_s \\ \Delta\mathbf{P}_l \end{bmatrix} = - \begin{bmatrix} \Delta\mathbf{g}^{P} \\ \Delta\mathbf{g}^{Q} \\ \Delta\mathbf{g}_{\text{conv}}^{P} \end{bmatrix} \tag{18}$$

where set $\mathbf{g}^P$ is composed of all the non-slack nodes' active power balance equations, and set $\mathbf{g}^Q$ is composed of all the non-voltage controlled nodes' reactive power balance equations, and $\mathbf{g}_{\text{conv}}^P$ represents the reactive power balance equations of all SOPs in the network. $\Delta\mathbf{g}^P = 0 - \mathbf{g}^P$, and $\Delta\mathbf{g}^Q$ and $\Delta\mathbf{conv}^P$ can be calculated similarly. Expression (18) can also be presented as $\mathbf{J}\Delta\mathbf{X} = -\Delta\mathbf{g}$ for simplicity. The overall power flow calculation for a given partition and corresponding recovered nodes is introduced in Appendix A. It is assumed that the relatively accurate topology information and line parameters are obtained based on the existing studies [27,28] before the power flow calculation, and the known measurements are also collected by high precision smart meters. Besides expressions (15)-(17), some usual constraints are also considered in the power flow calculation, including the nodal voltage limit, line flow limit, and CDG output limit.

4. Bi-objective Game Model and Solving Procedure

4.1. Bi-objective Non-cooperative Game Model

Let $\overline{G} = (Y_1 ..., Y_p, \overline{F}_1, \overline{F}_2, ..., \overline{F}_p)$ be a bi-objective game, where $Y_1, ..., Y_p$ are convex compact sets and $\overline{F}_1, \overline{F}_2, ..., \overline{F}_p$ represent the players' continuous vector payoff functions. The following theorem can be extracted [29]:

Theorem 1. *If for every $i \in \{1, 2, ..., p\}$, each component $F_i^k(y_1, ..., y_p)$, $k \in \{1, 2\}$ in the vector function $\overline{F}_i(y_1, ..., y_p)$ is a concave function with respect to y_i on Y_i for fixed $y_1, ..., y_{i-1}, y_{i+1}, ..., y_p$, then for bi-objective game $\overline{G} = (Y_1, ..., Y_p, \overline{F}_1, \overline{F}_2, ..., \overline{F}_p)$ there exists Pareto-Nash equilibria $y^{\star} = (y_1^{\star}, ..., y_p^{\star}) \in Y_1 \times Y_2 \times ... \times Y_p$.*

For the network partition problem in this paper, the variables are all discrete and the corresponding strategy sets $(X_1, X_2, ..., X_p)$ are finite. For the i-th player, $X_i = \{X_{i1}, X_{i2}, ..., X_{ir_i}\}$ represents all the partition schemes for the i-th CDG. Then the partition game is a finite discrete bi-objective game, which can be associated with a continuous bi-objective game $\overline{\overline{G}} = (Z_1, Z_2, ..., Z_p, \overline{f}_1, \overline{f}_2, ..., \overline{f}_p)$ by introducing mixed strategies $z_i = (z_{i1}, z_{i2}, ..., z_{ir_i}) \in Z_i$[29]. Z_i and $\overline{f}_i$ are presented as follows:

$$Z_i = \{z_i = (z_{i1}, z_{i2}, ..., z_{ir_i}) \in R^{r_i} | \sum_{j=1}^{r_i} z_{ij} = 1, \; z_{ij} \ge 0, j = \overline{1, r_i}\} \tag{19}$$

$$\overline{f}_i(*) = \left(f_i^1(*), f_i^2(*)\right), \; i = \overline{1, p} \tag{20}$$

where

$$\begin{aligned} & f_i^k(z_{11}, ..., z_{1r_1}, z_{21}, ..., z_{2r_2}, ..., z_{p1} ..., \quad z_{pr_p}) \\ & = \sum_{j_1=1}^{r_1} \sum_{j_2=1}^{r_2} ... \sum_{j_p=1}^{r_p} F_i^k(X_{1j_1}, ..., X_{ij_i}, ..., \quad X_{pj_p}) z_{1j_1} z_{2j_2} ... z_{pj_p} \\ & \qquad\qquad\qquad\qquad\qquad\qquad\qquad\qquad k = \{1, 2\}, i = \overline{1, p} \end{aligned} \tag{21}$$

It is not difficult to find that game $\overline{\overline{G}}$ satisfies the conditions in Theorem 1, and Pareto-Nash equilibrium $z^* = (z_{11}^*, ..., z_{1r_1}^*, z_{21}^*, ..., z_{2r_2}^*, ..., z_{p1}^*, ..., z_{pr_p}^*)$ exists. In order to calculate the Pareto-Nash equilibrium of the bi-objective game $\overline{\overline{G}}$, it can be transformed to a single objective game $G = (Z_1, Z_2, ..., Z_p, f_1, f_2, ..., f_p)$ by adding auxiliary parameters to the two objectives of each player. The new objective function for the single objective game is defined as:

$$f_i(*) = \alpha_{i,1} f_i^1(*) + \alpha_{i,2} f_i^2(*), \; i = \overline{1, p} \tag{22}$$

where

$$\alpha_{i,1} + \alpha_{i,2} = 1, \alpha_{i,1}, \alpha_{i,2} \ge 0, i = \overline{1, p} \tag{23}$$

If Nash equilibrium z^* is obtained for game G, then z^* is also the Pareto-Nash equilibrium solution for the bi-objective game $\overline{\overline{G}}$. The proof is provided in Appendix B of this paper.

4.2. Decentralized Realization of the Partition Game

For the partition game described in subsection IV-A, the players are the CDGs and the bi-objective functions are the weighted recovered load and the negative of the power loss. Before solving the game, $F_i^k(X_{1j_1}, ..., X_{ij_i}, ..., X_{pj_p})$ $(k = \{1, 2\}, i = \overline{1, p}, j_i = \overline{1, r_i})$ need to be calculated first, and all the possible strategies belonging to $X_1 \times X_2 \times ... \times X_p$ should be referred. Here, $F_i^k(X_{1j_1}, ..., X_{ij_i}, ..., X_{pj_p})$ is calculated using the local calculation of $F_i^k(X_{ij_i})(k = \{1, 2\}, i = \overline{1, p}, j_i = \overline{1, r_i})$, where the strategies of other CDGs are not considered.

$$F_i^k\left(X_{1j_1}, ..., X_{ij_i}, ..., X_{pj_p}\right) = \begin{cases} F_i^k(X_{ij_i}), & X_{1j_1}, ..., X_{ij_i}, ..., X_{pj_p} \text{ isvalid} \\ 0, & X_{1j_1}, ..., X_{ij_i}, ..., X_{pj_p} \text{ isinvalid} \end{cases} \tag{24}$$

For $X_{1j_1}, ..., X_{ij_i}, ..., X_{pj_p}$, it is valid when the partition for CDG i is not overlapped with any of its adjacent CDGs' partitions, while it is invalid when the partition for CDG i is overlapped with its adjacent CDGs'

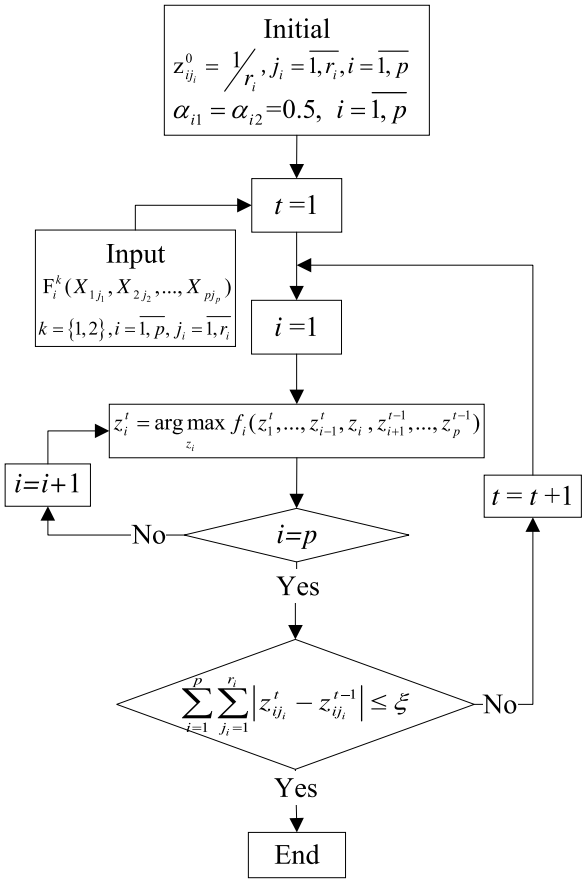

Fig. 5. Practical solving procedure of the game.

partitions. Two CDGs are adjacent if there is no other DGs on the path between these two CDGs. Taking path ① in Fig. 2 again as an example, if $n_{1i} \geq n_{3i}$, then the partitions of CDG-1 and CDG-3 overlap, and the corresponding strategy is invalid regardless of other CDGs' strategies. It is noteworthy that the validity of the strategies in (24) only depends on the adjacent CDGs of each CDG. Using this method, each CDG only needs to calculate its own objective function $F_i^k(X_{ij_i})$, $k = \{1,2\}, i = \overline{1,p}, j_i = \overline{1,r_i}$, which will reduce the calculation burden significantly, and also ensures the proposed model having good scalability. As the number of all the strategies for $X_{1j_1}, X_{2j_2}, ..., X_{pj_p}$ is $r_1 \times r_2 \times ... \times r_p$, the number of the calculations for $F_i^k(X_{ij_i}), k \in \{1,2\}, i \in \overline{1,p}, j_i \in \overline{1,r_i}$ is $r_1 + r_2 + ... + r_p$. Thus, the method in (24) can avoid a large number of invalid redundant calculations in $F_i^k(X_{1j_1}, X_{2j_2}, ..., X_{pj_p})$, $k = \{1,2\}, i = \overline{1,p}, j_i = \overline{1,r_i}$.

After all $F_i^k(X_{ij_i})$, $k = \{1,2\}, i = \overline{1,p}, j_i = \overline{1,r_i}$ are obtained, the game solving procedure based on the iterative method can be performed in a decentralized manner as shown in Fig. 5, where $\mathbf{z}_i^t = [z_{i1}^t, z_{i2}^t, ..., z_{ir_i}^t]$, and $\varepsilon = 1 \times 10^{-3}$. The optimization for $\mathbf{z}_i^t$ is performed locally in CDG i. The optimized $\mathbf{z}_i^t$ at i-th CDG is shared with its adjacent CDGs to guarantee the validity of the final Nash-Pareto equilibrium solution. All the CDGs linked together optimize and share their own strategies in turn at each iteration until the convergence condition in Fig. 5 is satisfied.

5. Case Studies

In this section, the proposed model is comprehensively validated and compared, and test scenarios of case studies are shown in Fig. 6. There are total 6 scenarios and 8 test cases in the test scenario diagram. The test cases 2 (the same with the case 4) and 5 can be found in subsection V-A, the test cases 1, 3, 6, 7, and 8 are conducted in subsections V-B, V-C, V-D, V-E, and V-F, respectively.

5.1. Solution of the Partition Game in 69-bus System

The proposed model is validated in the IEEE 69-bus system as shown in Fig. 2 in this subsection. The capacity of the CDG is set as 500 kW in

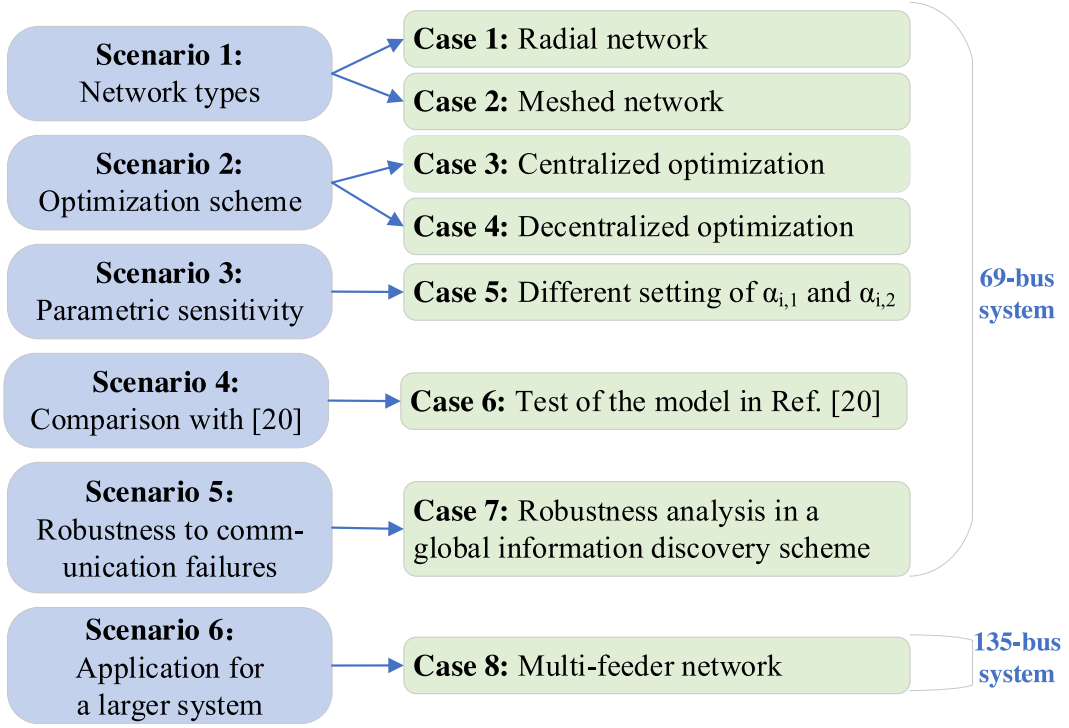

Fig. 6. The test scenarios for case studies.

Table 2
The objectives (kW) within different $\alpha_{i,1}$ and $\alpha_{i,2}$

$\alpha_{i,1}$	$\alpha_{i,2}$	Total weighted recovered load	Total power loss
1.0	0.0	17099	337
0.9	0.1	17162	323
0.8	0.2	17162	323
0.7	0.3	17162	323
0.6	0.4	17162	323
0.5	0.5	17162	237
0.4	0.6	17162	237
0.3	0.7	17162	237
0.2	0.8	17162	237
0.1	0.9	0.0	0.0
0.0	1.0	0.0	0.0

the test system, and the uncertainty of the PV and loads can be dealt with using a scenario reduction method in our previous work [30]. In this case study, we consider the worst-case scenario, where the average nodal active power is 200 kW (the importance levels of the load nodes are set as 1, 2 and 3 randomly), and the average PV output is 50 kW. The four paths in Fig. 2 (c) are involved in the optimization, and only the middle sections on these paths are considered in the decision variable domain for the test system. It is assumed that the remaining nodes on these four paths will be grouped with the nearest CDG. The middle sections of the four paths can be represented as path1=[46 45 44 43 42 41 40 39], path2=[15 14 13 12 11 10], path3=[22 23 24 25 26 27 65 64 63 62 61 60 59] and path4=[4 5 6 7 8], and the nodes' labeled numbers on the paths are $\overline{1,8}$, $\overline{1,6}$, $\overline{1,13}$, and $\overline{1,5}$, respectively. Then the strategies for each CDG are the node labeled numbers on these paths. As shown in Fig. 2 (c), CDG-1's strategies are related to path1, path2 and path3. Thus, the decision variables for CDG-1 are set as $[v_{1,1}, v_{1,2}, v_{1,3}]$. Similarly, the variables for CDG-2 and CDG-3 are set as $[v_{2,2}, v_{2,3}, v_{2,4}]$ and $[v_{3,1}, v_{3,4}]$, respectively. With such a variables setting, the partition of each CDG can be formed based on the routes from the node of CDG to the nodes these variables correspond to. Taking CDG-1 as an example, if $[v_{1,1}, v_{1,2}, v_{1,3}] = [2, 3, 4]$, then the partition of CDG-1 is formed by the route from node 17 to node 45, the route from node 17 to node 13, and the route from node 17 to node 25. The SOP between node 13 and node 21 will be involved in this partition as both nodes are assigned to this partition. Using the proposed method, the partition schemes for all CDGs can be determined, and the numbers of partition schemes for the three CDGs are 420, 240 and 28 (corresponding to r_1, r_2 and r_3), respectively.

After all the partition schemes are determined, the corresponding objective function values can be calculated based on the methods illustrated in Section III-B. The simulation is performed in the Matlab environment on a personal computer (PC) with Intel Core i5-8300H CPU @ 2.3-GHz and 16GB-RAM. For the first objective, the calculation time for each partition scheme is around 0.01 second 'intlinprog' function. For the second objective, the calculation time for each partition scheme is about 1 second based on the procedure described in Appendix A. For the unknown variables, the initial values for voltages and phase angles are set as 1 p.u. and 0, respectively, and the initial values of the unknown active powers and reactive powers for SOPs are set as 40% of total loads in the partition.

Given the objectives of all the partition schemes, the bi-objective game is solved based on the procedure in Fig. 5. It takes 4 iterations and 0.6 secend to obtain the equilibrium solution using Yalmip toolbox and Gurobi solver under the Matlab environment. The results of $\mathbf{z}_i^t$ in the iterative process are shown in TABLE 3. The variables of CDG-1 when $j_1 = 126$ is $[v_{1,1}, v_{1,2}, v_{1,3}] = [3, 1, 6]$, while those of CDG-2 and CDG-3 are $[v_{2,2}, v_{2,3}, v_{2,4}] = [2, 9, 3]$ ($j_2 = 30$) and $[v_{3,1}, v_{3,4}] = [4, 2]$ ($j_3 = 10$), respectively. The optimized partition scheme for each CDG is shown in Fig. 7 (b). The grey nodes in the figure represent the nodes that are not recovered, and the grey lines are the lines that are disconnected.

The objectives of the entire distribution network obtained from the proposed decentralized game theory based method with different $\alpha_{i,1}$ and $\alpha_{i,2}$ are listed in TABLE 2. According to the results, when $\alpha_{i,1} = 0$ or 0.1, both objectives are 0 as the power loss is overemphasized during the solving process in this case. When $\alpha_{i,1} = \overline{0.2, 0.9}$, the total weighted recovered loads are all 17,162 kW, and the power loss has a smaller value when $\alpha_{i,1} = \overline{0.2, 0.5}$. For the case with $\alpha_{i,1} = 1$, the total power loss is the largest among all the case. The results indicate that an appropriate setting of $\alpha_{i,1}$ and $\alpha_{i,2}$ is necessary to the performance of the partition optimization.

Table 3
The results of $\mathbf{z}_i^t$ in the iterative process

Partition	t=0	t=1	t=2	t=3
CDG-1	$z_{1,j_1} = 1/420$, $j_1 = \overline{1,420}$	$z_{1,j_1} = 1, j_1 = 61$ $z_{1,j_1} = 0, j_1 \neq 61$	$z_{1,j_1} = 1, j_1 = 126$ $z_{1,j_1} = 0, j_1 \neq 126$	$z_{1,j_1} = 1, j_1 = 126$ $z_{1,j_1} = 0, j_1 \neq 126$
CDG-2	$z_{2,j_2} = 1/240$, $j_2 = \overline{1,240}$	$z_{2,j_2} = 1, j_2 = 32$ $z_{2,j_2} = 0, j_2 \neq 32$	$z_{2,j_2} = 1, j_2 = 30$ $z_{2,j_2} = 0, j_2 \neq 30$	$z_{2,j_2} = 1, j_2 = 30$ $z_{2,j_2} = 0, j_2 \neq 30$
CDG-3	$z_{3,j_3} = 1/28$, $j_3 = \overline{1,28}$	$z_{3,j_3} = 1, j_3 = 10$ $z_{3,j_3} = 0, j_3 \neq 10$	$z_{3,j_3} = 1, j_3 = 10$ $z_{3,j_3} = 0, j_3 \neq 10$	$z_{3,j_3} = 1, j_3 = 10$ $z_{3,j_3} = 0, j_3 \neq 10$

5.2. Comparison with the Radial Network

In this section, the result of the network without SOPs (i.e., the radial network) will be compared with that of the meshed network with SOPs. The game solving process for the radial network partition is similar to Section V-A, and the partition results of the 2 different networks are shown in Fig. 7. The objective results and the nodal voltage profiles are shown in TABLE 4 and Fig. 8, respectively.

According to the optimized result in Fig. 8 and TABLE 4, the partition solution of CDGs with the radial network (as shown in Fig. 7 (a)) is different from that with the meshed network (as shown in Fig. 7 (b)). The total power loss within the meshed network (237 kW) is higher than that within the radial network (169 kW) as the involved SOPs usually cause extra power loss to some extent. However, the weighted recovered load within the meshed network is greater than that with the radial network, as the extra links from SOPs provide more flexibility and possibility for the partition. For the nodal voltage, the voltage curve of the meshed network also outperforms that of the radial network in general, especially at nodes 6∼8, 44∼46, 51 and 52. It can be seen that the nodal voltage at node 46 is 1 p.u. due to the voltage support from the SOP between node 15 and node 46, and the nodes with CDGs also hold 1 p.u. voltage. The curves in Fig. 8 are not continuous as several nodes are not included in the partitions.

5.3. Comparison with the Centralized Bi-objective Optimization

The results in previous subsections V-A and V-B are obtained through the proposed bi-objective game in a decentralized fashion. In this subsection, the centralized optimization as indicated in Fig. 1 (a) is performed and compared with the results of the proposed game. The centralized bi-objective optimization is performed in the Matlab environment on the same PC as mentioned in subsection V-A. It takes about 46 min to solve the partition optimization problem for the meshed network with SOPs, and the Pareto front is shown in Fig. 9. Selecting a trade-off solution (marked with a red circle) as the final result for the centralized optimization, the corresponding optimized variable values for CDG-1 is $[v_{1,1}, v_{1,2}, v_{1,3}] = [3, 2, 6]$, while those of CDG-2 and CDG-3 are $[v_{2,2}, v_{2,3}, v_{2,4}] = [2, 9, 4]$ and $[v_{3,1}, v_{3,4}] = [4, 2]$, respectively. The result is slightly different from that obtained with the game theory based method.

The comparison between the objective results of the decentralized game theory based method and the centralized optimization is shown in TABLE 5. The power loss with the game theory based method is very close to that with the centralized optimization. Meanwhile, the total recovered load with the decentralized game theory based method (17,162 kW) is about 99.6% of the value with the centralized

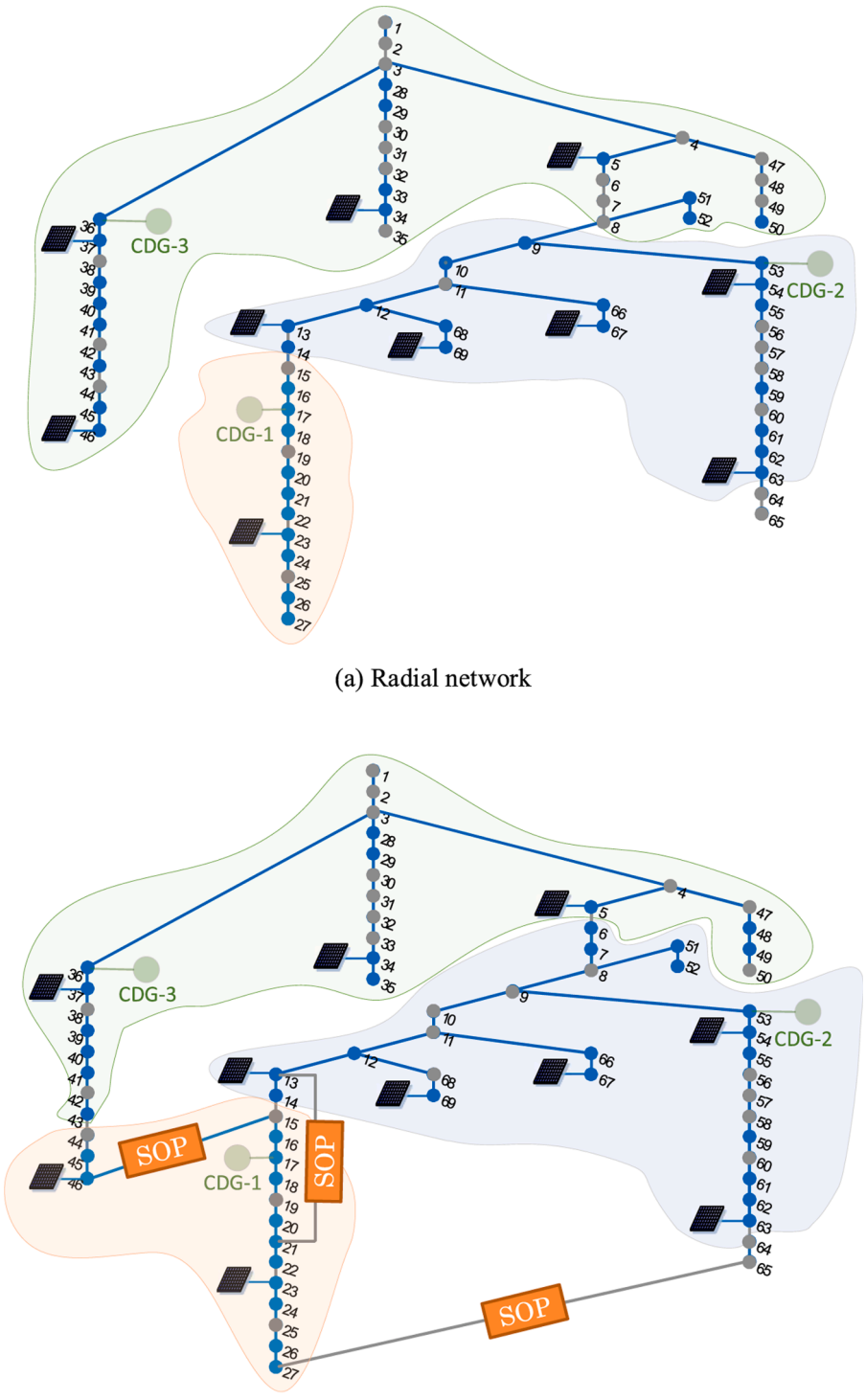

(a) Radial network

(b) Meshed network with SOP

Fig. 7. Partition optimization results of different networks.

Table 4
Results of objectives within radial network and meshed network with SOPs (kW)

Partitions	Weighted recovered load		Power loss	
	Radial	Meshed	Radial	Meshed
CDG-1	3327	3915	8	76
CDG-2	8995	9252	76	75
CDG-3	4333	3995	85	86
Total	16655	17162	169	237

optimization (17,224 kW). The results indicate that the proposed decentralized game theory based method can achieve very close objectives to the centralized optimization, while the time consumption of the solving process is much lower than the centralized optimization model.

5.4. Comparison with the Existing Studies

In this subsection, we will perform a test case based on a typical well-defined model considering SOPs in the distribution network partition

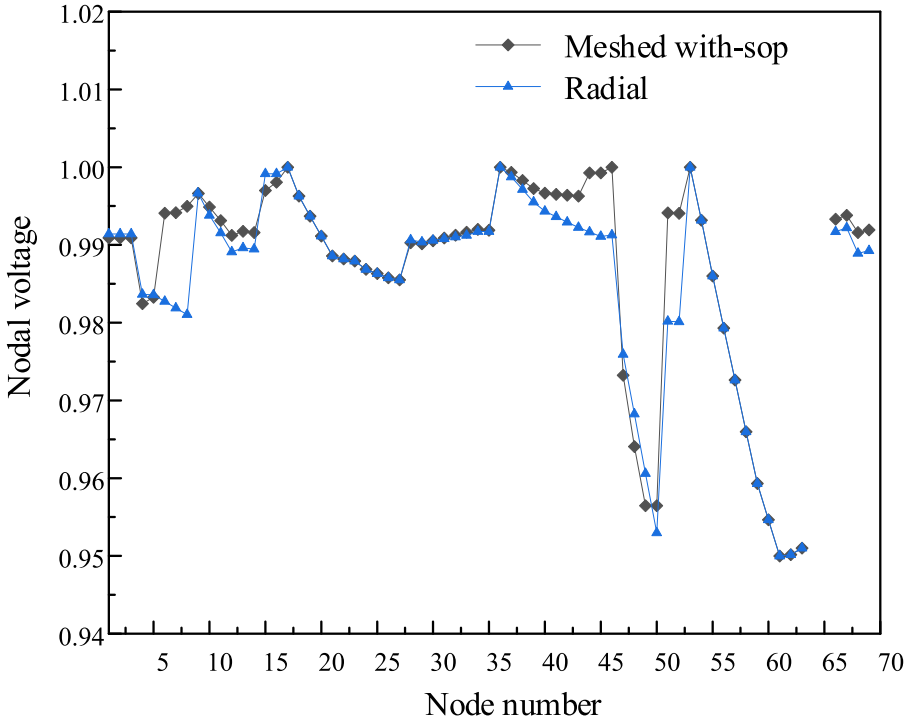

Fig. 8. Nodal voltage (p.u.) with different networks.

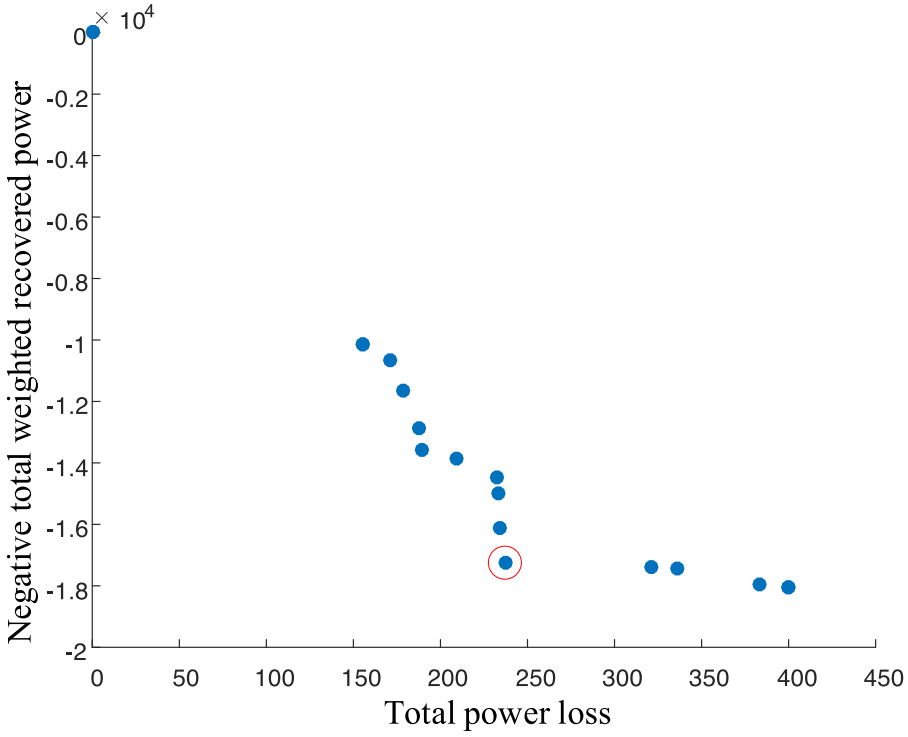

Fig. 9. Pareto front in the centralized optimization.

(reported in [24]). We apply the models in [24] on the IEEE 69-bus system as shown in Fig. 7 and compare the features of models from existing studies and our paper. The test case based on [24] takes about 120 seconds using Yalmip toolbox and Gurobi solver under the Matlab environment, and the result is shown in Fig. 10. The partition result is a bit different with that in Fig. 7 (b), and the weighted recovered load corresponding to Fig. 10 is 18012 kW, which is slightly higher than the result of centralized model (17224 kW) as shown in TABLE 5. As in [24],

Table 5
Results of objectives with the game and the centralized optimization (kW)

Partitions	Weighted recovered load		Power loss	
	Centralized	Game	Centralized	Game
CDG-1	4035	3915	76.3	76.1
CDG-2	9193	9252	75.2	74.7
CDG-3	3995	3995	85.9	85.9
Total	17224	17162	237.4	236.7

the power loss was not considered in the objectives, and the mathematical models for SOPs and power flow calculation are both different with the ones in our paper.

A more detailed comparison of the model features is presented in TABLE 6, with another study [9] listed as well which utilizes a decentralized optimization model. According to TABLE 6, our paper adopted a more detailed SOP model considering the inner structure of converters. For the power flow model, Refs.[24] and [10] utilized the Distflow and linearized Distflow models, respectively. Both of them are approximate methods. The Newton-Raphson method is adopted in our paper to achieve more precise solution as the power losses obtained are more accurate. Meanwhile, the Distflow based models assume radial network topologies. In contrast, benefited from the exact nonlinear power flow calculation, our proposed model is also applicable to the cases where there are loops in the partitions, and this feature is not possessed in other existing studies.

5.5. Robustness Analysis to Communication Failures

The global information discovery scheme mentioned in Section 2 could be achieved by local communications without the extra infrastructure support as stated in [10], and it is adopted in our work to support the proposed model. The corresponding communication network for the IEEE 69-bus test system is structured as shown in Fig. 11. The regional agent (RA) is installed in the node with CDG, and has a high ability in computation to calculate the objectives of strategies and optimize the decisions in the game solving process. The local agent (LA) represents a individual device (a switch, a SOP on a line, or a node controller) or a group of devices, and the case for a LA in Fig. 11 is the latter one.

As shown in Fig. 11, any single failure on the communication link will not influence the global information discovery, and the failures on two communication links may cause the isolation of one LA in the worst case (the both failures occur on the only two communication links of one LA). When there are 3 communication links are damaged, there may be one RA or LA being isolated in the worst case (all the three failures occur on the only three communication links of one LA/RA). The analyses for other failure cases are similar with the above cases, and they may cause the isolation of RA/LAs, or even the separation of the overall communication network. However, in our proposed self-organized framework, the isolated RA/LAs or the separated communication network will not cause the paralysis of the whole system, and the remaining communication network could still support the network partition task between the nodes being able to communicate using the information discovery. However, in the centralized optimization model, which could still adopt the communication network as shown in Fig. 11(which means that the communication costs on infrastructures are the same between this two optimization models), the failure at the central controller will cause the

Table 6
The comparison of model features with the existing studies

Items	Ref. [24]	Ref. [10]	Our paper
SOP model	Inner structure not considered	No SOP	Inner structure considered
Power flow model	Distflow	Linearized Distflow	Newton-Raphson
Optimization scheme	Centralized	Decentralized	Decentralized
Optimization objectives	Recovered load	Weighted recovered load	Weighted recovered load & Power loss
Topology related variables	State of lines	State of lines	Labeled numbers on the linking paths
Applicable network structure	Radial	Radial	Radial & Looped
Robustness to communication failures	Weak	Strong	Strong

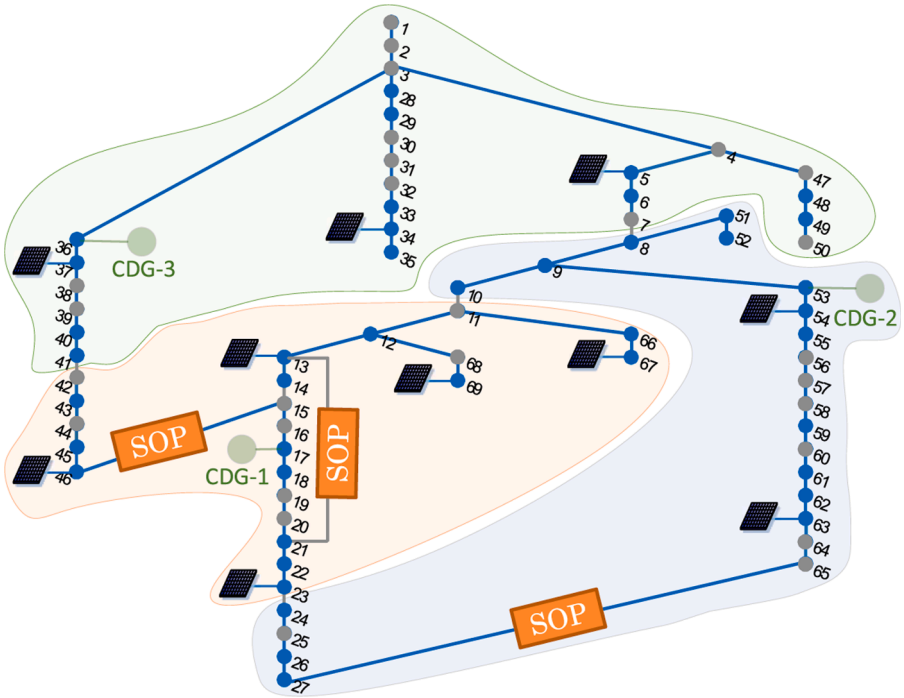

Fig. 10. Partition optimization results with the model in Ref. [20].

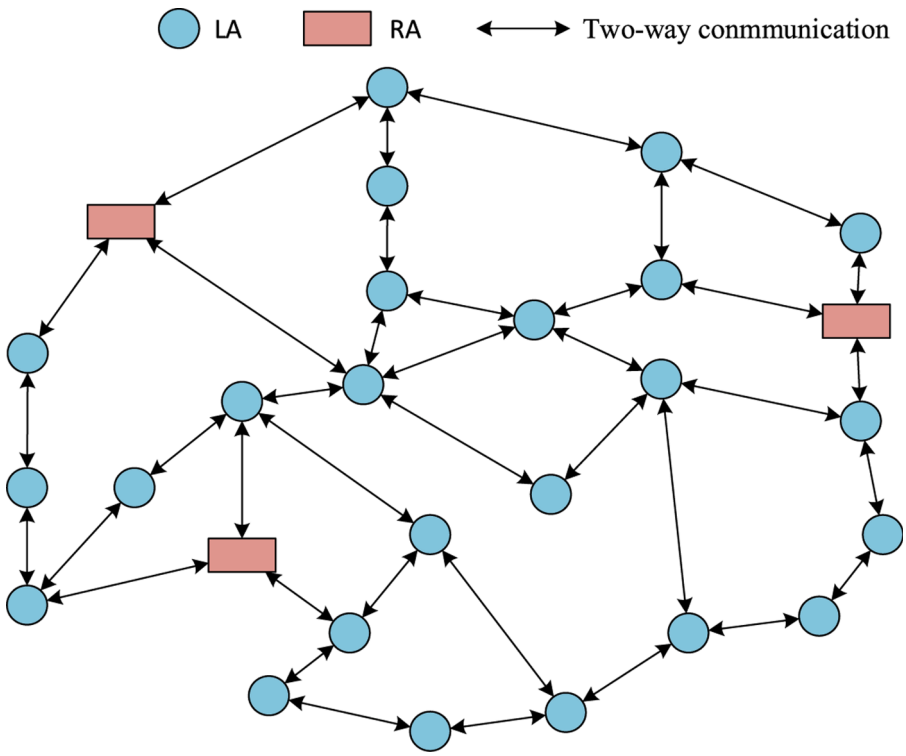

Fig. 11. Communication network for global information discovery

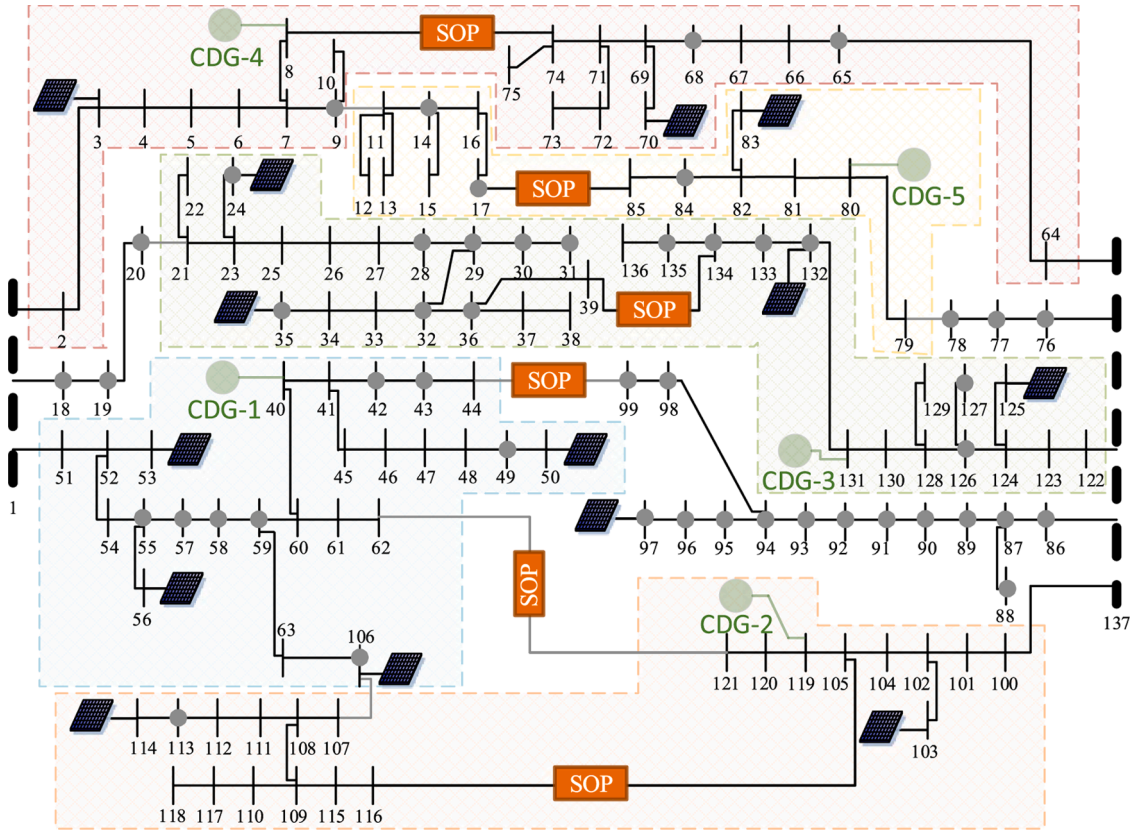

Fig. 12. Partition optimization results of the multi-feeder distribution system

interrupt of the overall optimization process for the network partition.

5.6. Application in Multi-feeder Distribution Systems

The results in Fig. 7 are based on a single-feeder distribution network, and in this section the proposed model is verified in a 135-bus multi-feeder distribution system as shown in Fig. 12 [31]. It is assumed that the bus bars at the node 1 and node 137 have been damaged in the extreme event, and the feeders cannot connect with each other through the bus-bars. Generally, in a multi-feeder distribution system, only a limited number of feeders are connected together through SOPs (normally-opened tie switches in the case without SOPs), to make the system operation and control clearer and easier. For the distribution system in Fig. 12, there are 8 feeders in total, and the total load to be recovered is around 20 MW. The first feeder connected to node 1, the first and second feeders connected to node 137 are linked through 2 SOPs, the second feeder connected to node 1 and the third feeder connected to node 137 are linked, and the rest feeders are linked. That means the system could be regarded as 3 relatively independent subsystems, named subsystem 1, 2, and 3. The similar realization process and initial value settings in the 69-bus system are adopted in each subsystem, and the partition result is shown in Fig. 12, and about half of the load is recovered (the unrecovered nodes and disconnected lines are marked using grey color).

For each partition in this multi-feeder distribution system, the calculation time for the first objective and the second objective are about 0.04 and 1 second, respectively. It takes 4, 3 and 3 iterations to obtain the equilibrium solution for subsystem 1,2, and 3 in Fig. 12, respectively. And the game solving processes are all finished within 1 second. We can find that the calculation time for the multi-feeder system is not significantly longer than that for a single-feeder system. It is not difficult to infer that the proposed model could be adopted in a much larger distribution system without an obvious increase in calculation time, as the calculations of the two objectives for all the partition schemes are conducted in each CDG just involving the adjacent nodal information (the adjacent nodes refer to the nodes between this CDG and its adjacent CDGs), and this process could be simultaneously proceeded in all the CDGs, which means the total calculation time will not be increased significantly. For the game solving process, it is also not time-consuming as the game features finite strategies as shown in the 69-bus system and the 135-bus multi-feeder system. The above features ultimately guarantee the scalability of the proposed models in the application.

6. Conclusions

Resilience enhancement of the distribution network after a severe power outage has attracted extensive attention from the government, industry and academia in recent years. In this study, a self-organized network partition framework is proposed for the distribution network with DGs and SOPs from the game theoretic perspective. The labeled numbers of nodes on the paths between two adjacent CDGs are used as the decision variables in the partition formation to avoid a large number of invalid partition schemes. Two objectives including the weighted recovered load and power loss are considered in the partition optimization, and the exact AC power flow model is utilized to determine the power loss, where a detailed SOP model is integrated. A discrete bi-objective game is modeled to solve the partition optimization, and a decentralized method is designed to solve the game only relying on the local communications, which is more suitable for the cases under extreme events compared with the centralized methods. Finally, a numerical test is performed on the IEEE 69-bus distribution systems and a 135-bus multi-feeder system to verify the proposed partition model. According to the results, the proposed method is applicable for both radial and meshed distribution network topology. The comparison between the proposed decentralized game theory model and the centralized optimization model shows that the objectives for the partitions are very close with both methods, while the proposed game theory based method has much lower time consumption than centralized optimization. The proposed model is also compared with other existing studies in this field, and the feature comparison has been performed in the case study. The robustness analysis to communication failures shows that the proposed decentralized model is more reliable when failures occur in the communication network compared with a centralized optimization model. The proposed model has also been applied in a larger multi-feeder distribution network, and it shows that the local communication and decentralized implementation process ensure the proposed model possesses good scalability in practical application. In the future, the operational measures dealing with local outages caused by man-made disasters such as cyberattacks can be further studied considering the advantages of SOPs.

CRediT authorship contribution statement

Li Ma: Conceptualization, Methodology, Software, Validation, Formal analysis, Investigation, Data curation, Writing – original draft, Visualization. **Lingfeng Wang:** Conceptualization, Methodology, Resources, Writing – review & editing, Supervision, Project administration, Funding acquisition. **Zhaoxi Liu:** Conceptualization, Writing – review & editing.

Declaration of Competing Interest

The authors declare that they have no known competing financial interests or personal relationships that cdocould have appeared to influence the work reported in this paper.

Acknowledgments

This work was supported in part by the U.S. National Science Foundation Industry/University Cooperative Research Center on Grid-connected Advanced Power Electronic Systems (GRAPES) under Award GR-18-06.

Appendix A. Power Flow Calculation Procedure

Given a partition scheme and the corresponding recovered nodes, the steps of the overall power flow calculation procedure are shown in Fig. 13.

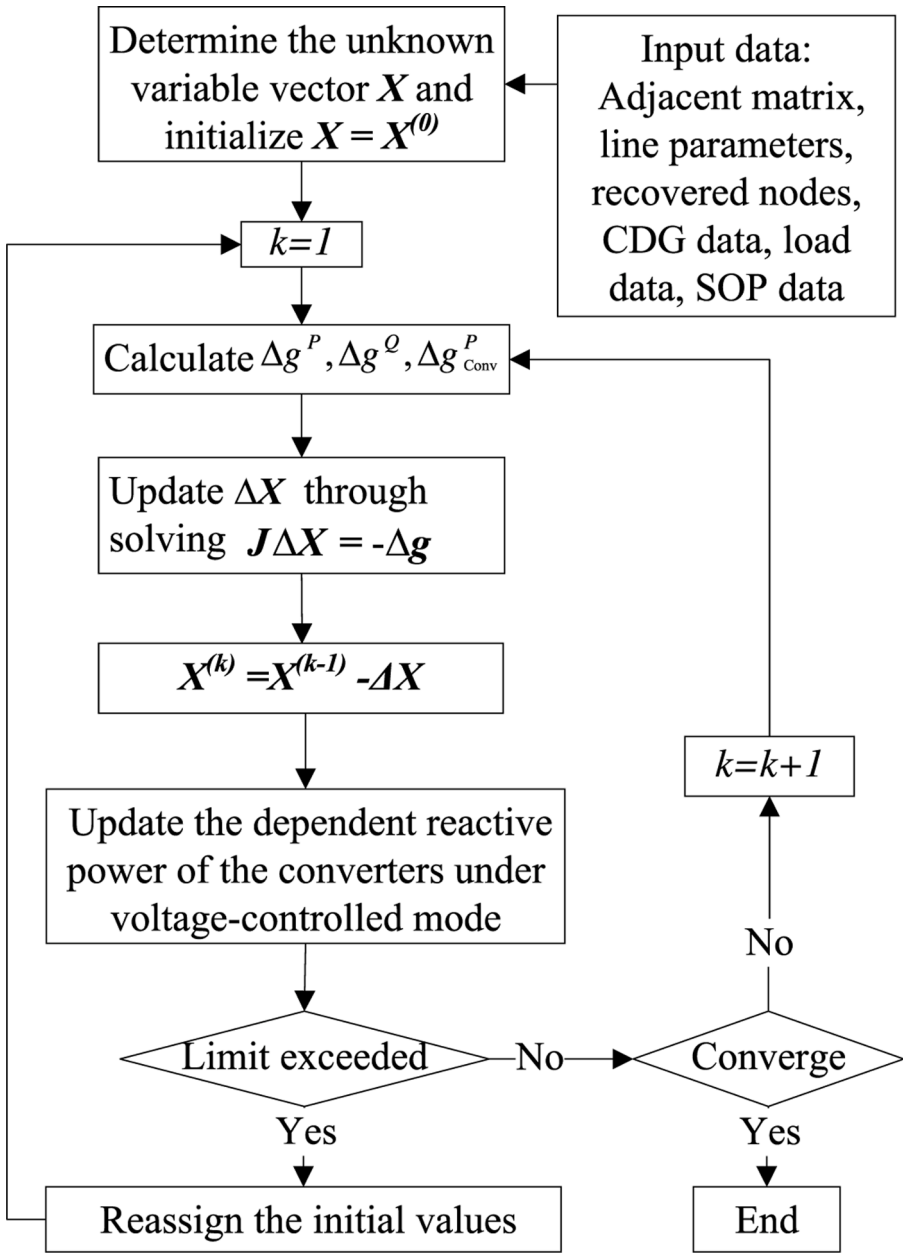

Fig. 13. The procedure of power flow calculation with SOPs.

Appendix B. Proof of the Equilibrium Solution

Theorem 2. *If the strategy spaces are nonempty compact convex subsets of an Euclidean space, and the payoff functions are continuous and quasi-concave in a game, there exists a pure-strategy Nash equilibrium [32].*

According to Theorem 2, for the single objective game $G = (Z_1, Z_2, ..., Z_p, f_1, f_2, ..., f_p)$*, there exists a Nash equilibrium* $z^* = [z_1^*, z_2^*, ..., z_p^*]$.

$$f_i\left(z_1^*, ..., z_i, ..., z_p^*\right) \le f_i\left(z_1^*, ..., z_i^*, ..., z_p^*\right), z_i \in Z_i, i = \overline{1,p} \tag{25}$$

The next step is to prove that z^* *is also the Pareto-Nash equilibrium solution for bi-objective game* $\overline{\overline{G}} = (Z_1, Z_2, ..., Z_p, \bar{f}_1, \bar{f}_2, ..., \bar{f}_p)$*, where* $\bar{f}_i(*) = (f_i^1(*), f_i^2(*)), i = \overline{1,p}$*. By definition, it is equivalent to the fact that the following two conditions (a) and (b) hold simultaneously:*

(a) If $f_i^2(z_1^*, ..., z_i, ..., z_p^*) = f_i^2(z_1^*, ..., z_i^*, ..., z_p^*)$*, then*

$$f_i^1\left(z_1^*, ..., z_i, ..., z_p^*\right) \le f_i^1\left(z_1^*, ..., z_i^*, ..., z_p^*\right), z_i \in Z_i, i = \overline{1,p} \tag{26}$$

(b) If $f_i^1(z_1^*, ..., z_i, ..., z_p^*) = f_i^1(z_1^*, ..., z_i^*, ..., z_p^*)$*, then*

$$f_i^2\left(z_1^*, ..., z_i, ..., z_p^*\right) \le f_i^2\left(z_1^*, ..., z_i^*, ..., z_p^*\right), z_i \in Z_i, i = \overline{1,p} \tag{27}$$

Taking case (a) as an example, for any $\alpha_{i,1}, \alpha_{i,2}$ that satisfy the condition (23), as $f_i(*) = \alpha_{i,1} f_i^1(*) + \alpha_{i,2} f_i^2(*), i = \overline{1,p}$,

$$\begin{aligned} &\alpha_{i,1} f_i^1\left(z_1^*, ..., z_i, ..., z_p^*\right) + \alpha_{i,2} f_i^2\left(z_1^*, ..., z_i, ..., z_p^*\right) \\ &\le \alpha_{i,1} f_i^1\left(z_1^*, ..., z_i^*, ..., z_p^*\right) + \alpha_{i,2} f_i^2\left(z_1^*, ..., z_i^*, ..., z_p^*\right) \\ &z_i \in Z_i, i = \overline{1,p} \end{aligned} \tag{28}$$

As $f_i^2(z_1^*, ..., z_i, ..., z_p^*) = f_i^2(z_1^*, ..., z_i^*, ..., z_p^*)$, $f_i^2(*)$ can be deleted from both sides, then

$$\begin{aligned} &\alpha_{i,1} f_i^1\left(z_1^*, ..., z_i, ..., z_p^*\right) \\ &\le \alpha_{i,1} f_i^1\left(z_1^*, ..., z_i^*, ..., z_p^*\right),\ z_i \in Z_i, i = \overline{1,p} \end{aligned} \tag{29}$$

As $\alpha_{i,1} \ge 0$, it can be derived that

$$\begin{aligned} &f_i^1\left(z_1^*, ..., z_i, ..., z_p^*\right) \\ &\le f_i^1\left(z_1^*, ..., z_i^*, ..., z_p^*\right),\ z_i \in Z_i, i = \overline{1,p} \end{aligned} \tag{30}$$

This completes the proof that (a) holds, and case (b) can be proved similarly. Thus, it is proved that z^* is also the Pareto-Nash equilibrium of bi-objective game $\overline{\overline{G}}$.

References

[1] W. House, Economic benefits of increasing electric grid resilience to weather outages, Washington, DC: Executive Office of the President (2013).
[2] D.U. Case, Analysis of the cyber attack on the ukrainian power grid, Electricity Information Sharing and Analysis Center (E-ISAC) 388 (2016).
[3] Critical infrastructure resilience: Final report and recommendations, National Infrastructure Advisory Council, 2009.
[4] D.K. Mishra, M.J. Ghadi, A. Azizivahed, L. Li, J. Zhang, A review on resilience studies in active distribution systems, Renewable and Sustainable Energy Reviews 135 (2021) 110201.
[5] W. Yuan, J. Wang, F. Qiu, C. Chen, C. Kang, B. Zeng, Robust optimization-based resilient distribution network planning against natural disasters, IEEE Transactions on Smart Grid 7 (6) (2016) 2817–2826.
[6] S. Ma, B. Chen, Z. Wang, Resilience enhancement strategy for distribution systems under extreme weather events, IEEE Transactions on Smart Grid 9 (2) (2016) 1442–1451.
[7] J. Zhao, H. Niu, X. Zhang, Island partition of distribution network with microgrid based on the energy at risk, IET Generation, Transmission & Distribution 11 (4) (2017) 830–837.
[8] Z. Wang, J. Wang, Self-healing resilient distribution systems based on sectionalization into microgrids, IEEE Transactions on Power Systems 30 (6) (2015) 3139–3149.
[9] D.N. Trakas, N.D. Hatziargyriou, Optimal distribution system operation for enhancing resilience against wildfires, IEEE Transactions on Power Systems 33 (2) (2017) 2260–2271.
[10] C. Chen, J. Wang, F. Qiu, D. Zhao, Resilient distribution system by microgrids formation after natural disasters, IEEE Transactions on smart grid 7 (2) (2015) 958–966.
[11] A. Sharma, D. Srinivasan, A. Trivedi, A decentralized multiagent system approach for service restoration using dg islanding, IEEE Transactions on Smart Grid 6 (6) (2015) 2784–2793.
[12] Y. Zeng, C. Qin, J. Liu, X. Xu, Coordinating multiple resources for enhancing distribution system resilience against extreme weather events considering multi-stage coupling, International Journal of Electrical Power & Energy Systems 138 (2022) 107901.
[13] Y. Lin, Z. Bie, Tri-level optimal hardening plan for a resilient distribution system considering reconfiguration and dg islanding, Applied Energy 210 (2018) 1266–1279.
[14] S. Lei, C. Chen, H. Zhou, Y. Hou, Routing and scheduling of mobile power sources for distribution system resilience enhancement, IEEE Transactions on Smart Grid 10 (5) (2018) 5650–5662.
[15] J. Kim, Y. Dvorkin, Enhancing distribution system resilience with mobile energy storage and microgrids, IEEE Transactions on Smart Grid 10 (5) (2018) 4996–5006.
[16] A. Shahbazi, J. Aghaei, S. Pirouzi, T. Niknam, M. Shafie-khah, J.P. Catalão, Effects of resilience-oriented design on distribution networks operation planning, Electric Power Systems Research 191 (2021) 106902.
[17] Z. Bie, Y. Lin, G. Li, F. Li, Battling the extreme: A study on the power system resilience, Proceedings of the IEEE 105 (7) (2017) 1253–1266.
[18] A.A. Bayod-Rújula, Future development of the electricity systems with distributed generation, Energy 34 (3) (2009) 377–383.
[19] M.A. Elsadd, T.A. Kawady, A.-M.I. Taalab, N.I. Elkalashy, Adaptive optimum coordination of overcurrent relays for deregulated distribution system considering parallel feeders, Electrical Engineering (2021) 1–19.
[20] J.M. Bloemink, T.C. Green, Increasing distributed generation penetration using soft normally-open points. IEEE PES General Meeting, IEEE, 2010, pp. 1–8.
[21] S. Giannelos, I. Konstantelos, G. Strbac, Option value of soft open points in distribution networks. 2015 IEEE Eindhoven PowerTech, IEEE, 2015, pp. 1–6.
[22] P. Li, H. Ji, C. Wang, J. Zhao, G. Song, F. Ding, J. Wu, Coordinated control method of voltage and reactive power for active distribution networks based on soft open point, IEEE Transactions on Sustainable Energy 8 (4) (2017) 1430–1442.
[23] C. Long, J. Wu, L. Thomas, N. Jenkins, Optimal operation of soft open points in medium voltage electrical distribution networks with distributed generation, Applied Energy 184 (2016) 427–437.
[24] H. Ji, C. Wang, P. Li, G. Song, J. Wu, Sop-based islanding partition method of active distribution networks considering the characteristics of dg, energy storage system and load, Energy 155 (2018) 312–325.
[25] R.B. Myerson, Game theory, Harvard university press, 2013.
[26] Q. Nguyen, G. Todeschini, S. Santoso, Power flow in a multi-frequency hvac and hvdc system: Formulation, solution, and validation, IEEE Transactions on Power Systems 34 (4) (2019) 2487–2497.
[27] J. Yu, Y. Weng, R. Rajagopal, Patopa: A data-driven parameter and topology joint estimation framework in distribution grids, IEEE Transactions on Power Systems 33 (4) (2017) 4335–4347.
[28] J. Zhang, Y. Wang, Y. Weng, N. Zhang, Topology identification and line parameter estimation for non-pmu distribution network: A numerical method, IEEE Transactions on Smart Grid 11 (5) (2020) 4440–4453.
[29] D. Lozovanu, D. Solomon, A. Zelikovsky, Multiobjective games and determining pareto-nash equilibria, Buletinul Academiei de Ştiinţe a Republicii Moldova. Matematica (3) (2005) 115–122.
[30] L. Ma, N. Liu, J. Zhang, L. Wang, Real-time rolling horizon energy management for the energy-hub-coordinated prosumer community from a cooperative perspective, IEEE Transactions on Power Systems 34 (2) (2018) 1227–1242.
[31] J.R. Mantovani, F. Casari, R.A. Romero, Reconfiguração de sistemas de distribuição radiais utilizando o critério de queda de tensão, Controle and Automacao (2000) 150–159.
[32] G. Debreu, A social equilibrium existence theorem, Proceedings of the National Academy of Sciences 38 (10) (1952) 886–893.